

SYK model with an extra diagonal perturbation: phase transition in the eigenvalue spectrum

Shuang Wu¹

Shanghai Center for Complex Physics, School of Physics and Astronomy, Shanghai Jiao
Tong University, Shanghai 200240, China

Abstract

We study the SYK model with an extra constant source, i.e. a constant matrix or equivalently a diagonal matrix with only one non-zero entry λ_1 . By using methods from analytic combinatorics [9], we find exact expressions for the moments of this model. We further prove that the spectrum of this model can have a gap when $\lambda_1 > \lambda_1^c$, thus exhibiting a phase transition in λ_1 . In this case, a single isolated eigenvalue splits off from SYK's eigenvalues distribution. We located this single eigenvalue by analyzing the singular behavior of a supercritical functional composition scheme. In certain limit our results recover the ones of random matrices with non-zero mean entries.

1 Introduction

Considering the SYK model plus a diagonal matrix with only one non-zero entry λ_1 :

$$\begin{aligned} H &:= H_{\text{SYK}} + \wedge \\ &= i^{p(p-1)/2} \sum_{1 \leq i_1 < i_2 < \dots < i_p \leq N} J_{i_1, i_2, \dots, i_p} \psi_{i_1} \psi_{i_2} \dots \psi_{i_p} + \begin{bmatrix} \lambda_1 & 0 \\ & \ddots \\ 0 & 0 \end{bmatrix} \end{aligned} \quad (1)$$

the first part above is just the usual SYK [1–3] Hamiltonian with p ψ_j interacting Majorana fermions among N Majorana fermions satisfying $\{\psi_i, \psi_j\} = 2\delta_{i,j}$. The factor i in front of (1) is introduced to keep H_{SYK} Hermitian. J_{i_1, i_2, \dots, i_p} are random coupling satisfying

$$\langle J_{i_1, i_2, \dots, i_p}^2 \rangle_J = \frac{1}{\binom{N}{p}} \quad (2)$$

where $\langle \dots \rangle_J$ represents the ensemble average over the random couplings J ². We choose this scaling to simplify the calculation, with (2), we normalize the trace of SYK Hamiltonian $\langle \text{tr} H_{\text{SYK}}^2 \rangle_J = 1$ ³. Therefore, moments calculation can be reduced to a combinatorial

¹scholes89@sjtu.edu.cn

²Note that the variance (2) is not a common choice. In the double scaled limit (3), it is different from the usual SYK conventions only by a constant factor [5]. This is a normalization factor which corresponds to the number of terms under the sum over the index sets in (1) and is chosen to keep the spectrum of order 1.

³trace operator in this paper is normalized as $\text{tr} 1 = 1$.

counting problem [5]. The last term \mathbb{A} in (1) is a $2^{\lfloor N/2 \rfloor} \times 2^{\lfloor N/2 \rfloor}$ diagonal matrix with only one non-zero element λ_1 . Since the SYK Hamiltonian is a large sparse matrix, (1) can also be treated as a matrix. We note that (1) can be understood as a special case of an SYK-model deformed by a random Hamiltonian diagonal in Fock space [4]. The model in [4] is non-ergodic, namely its spectral statistics is of Wigner-Dyson type, whereas its wave functions are non-uniformly distributed over Fock space. It serves as a toy model to study the non-ergodic extendedness in quantum chaotic systems. The perturbation in this model is introduced by a diagonal term ⁴, which is a sum over projectors onto the occupation number eigenstates $|n\rangle = |n_1, n_2, \dots, n_k, \dots\rangle$, with $n_i = 0, 1$. Each state attached to a coefficient v_n as a random variable with respect to a box distribution. In their case, the spectral statistics are of Wigner-Dyson type. Now in our case, \mathbb{A} can be understood as a special projection of one eigenstate, which is the ground state $|1, 0, 0, \dots\rangle$ coupled with a fixed eigenvalue λ_1 . The crucial difference between (1) and the model in [4] is that we fixed the value of λ_1 ; they choose a random variable v_n to attach the occupied state $|n\rangle$. Thus, there is a fundamental difference between the spectral densities of these two model. Only a fixed coefficient can bring the largest eigenvalue separation into the spectrum. The reason is that there is a phase transition in λ_1 , only when λ_1 passes its critical value, a single eigenvalue splits off from the main spectrum of (1). This is why the model in [4] has no such separation in its spectral density.

There are two motivations of studying this model. The first one is to find an SYK-like model which has similar spectral properties of random matrix with non-zero mean entries [6,7]. Like random matrix, a small rank perturbation of SYK can affect significantly the limiting properties of the spectrum as the system size goes to infinity. Depending on the values of λ_1 we put in, we can have a separation of the largest eigenvalue, thus there is a phase transition in λ_1 just like the random matrix case. The other reason for addressing this rather simple perturbatively model arises from the deep connection between the phase transitions in physics and the asymptotic analysis of a critical composition scheme of combinatorial structures (i.e. when a class of combinatorial structures can be decomposed into more basic building blocks, its generating function is then a functional composition of those of the building blocks. It is critical when both its and the building blocks generators are simultaneously singular). See [8] for more recent discussion about this connection.

In this work, we first map the ensemble averaging moments calculation of (1) into a counting problem of complex combinatorial structures. Furthermore, the class of these structures can be obtained by combining operators of more well-studied classes of substructures. Any specification of a constructible class translates directly into its generating function equations. Then, we can enumerate this decomposable class via its generating function. In our case, the specific class is constructed by a pointing operator of a labeled cyclic class of certain rooted substructures. In section 2 we will give a brief introduction about how to construct a decomposable class of combinatorial structures by using specific operations which will be used in our work. We refer [9] for detailed definitions.

In the following, we are interested in studying the distribution of eigenvalues of (1),

⁴in [4], they call it Fock-space diagonal operator $\tilde{H}_v = \gamma \sum_n v_n |n\rangle \langle n|$.

in the doubled scaled limit [5, 11, 14]

$$N \rightarrow \infty, \quad \lambda = \frac{2p^2}{N} = \text{fixed}. \quad (3)$$

First of all, define $\Psi_\alpha = i^{p(p-1)/2} \prod_{i=1}^p \psi_{i_i}$ as the product of p Majorana fermions, α represents an index set as $\alpha = \{i_1, i_2 \dots i_p\}$ which satisfy

$$\Psi_\alpha^2 = \mathbb{1}, \quad \Psi_\alpha \Psi_\beta = (-1)^{c_{\alpha\beta} + p} \Psi_\beta \Psi_\alpha \quad (4)$$

where $c_{\alpha\beta} = |\alpha \cap \beta|$ is the number of common indices in the sets α and β . In the doubled scaled limit, $c_{\alpha\beta}$ follows a Poisson distribution with mean p^2/N [5]. In the following we assume p is always even. In addition, we introduce a new variable q as a factor to count the exchange between any two Ψ in this double scaling limit (3)

$$\begin{aligned} \Psi_\alpha \Psi_\beta &= q \Psi_\beta \Psi_\alpha \quad \forall \alpha, \beta \\ \text{with } q &:= \sum_{c_{\alpha\beta}=0}^{\infty} \frac{(p^2/N)^{c_{\alpha\beta}}}{c_{\alpha\beta}!} (-1)^{c_{\alpha\beta}} \exp(-p^2/N) = \exp(-\lambda) \end{aligned} \quad (5)$$

therefore $q \in [0, 1]$. We also assume that no three sets of fermions can have common elements at the same time $|\alpha \cap \beta \cap \gamma| = 0$. This is equivalent to assuming that no three chords in a diagram intersect at the same point. Finally, we should point out that though our results are computed in the limit (3), they are also have a very good agreement with fixed finite p cases (see similar situation in [11, 12]). The trick is with finite p , one has to change the notation of q in (5) to

$$\tilde{q}(p) = \sum_{c=0}^p (-1)^c \binom{p}{c} \binom{N-p}{p-c} \quad (6)$$

1.1 Results

The main results in the paper are the following.

Define m_p as the ensemble averaging moments of the (1) extracted by ensemble averaging moments of the SYK Hamiltonian

$$\begin{aligned} m_p &= 2^{\lfloor N/2 \rfloor} \left(\langle \text{tr} H^p \rangle_J - \langle \text{tr} H_{\text{SYK}}^{2\lfloor p/2 \rfloor} \rangle_J \right) \\ m_p &= \sum_{j=0}^{\lfloor \frac{p-1}{2} \rfloor} \lambda_1^{p-2j} \frac{p}{p-2j} \sum_{\substack{k_1, k_2, \dots, k_j \geq 0 \\ k_1 + 2k_2 + \dots + jk_j = j}} \binom{p-2j}{k_1, k_2, \dots, k_j, p-2j - \sum_{l=1}^j k_l} \prod_{i=1}^j \text{RT}(i, q)^{k_i} \end{aligned} \quad (7)$$

where $\lfloor \frac{p-1}{2} \rfloor$ denotes the integerpart of $\frac{p-1}{2}$. $\text{RT}(i, q) = \langle \text{tr} H_{\text{SYK}}^{2i} \rangle_J$ is the Riordan-Touchard formula, which counts the ensemble averaging $2i$ -th normalized moment of SYK in the

double scaled limit [5, 11, 14]. We notice that when $q = 0$, $\text{RT}(i, 0)$ is the i -th Catalan number, (7) can be simplified dramatically, it recovers the moments of the eigenvalue density of a random matrix with a finite mean [7] (see appendix for the proof). By rearranging the second sum in (7), we get

$$m_p = \sum_{j=0}^{\lfloor \frac{p-1}{2} \rfloor} \lambda_1^{p-2j} \frac{p}{p-2j} \sum_{\substack{l=1 \\ k_1+k_2+\dots+k_l=j}}^j \binom{p-2j}{l} \prod_{i=1}^l \text{RT}(k_i, q) \quad (8)$$

the second sum in (8), is a sum over all compositions of integer j into l parts. It should be noted that the expressions above are not special, other non-commutative models also have these kinds of structures (for ex, Hofstadter model [15]).

We prove the generating function to be

$$\sum_{p \geq 1} m_p z^p = z \frac{d}{dz} \log \frac{1}{1 - \lambda_1 z R(z, q)} \quad (9)$$

where $R(z, q)$ is defined as the generation function of $\text{RT}(i, q)$

$$R(z, q) := \sum_{i \geq 0} \text{RT}(i, q) z^{2i} = \frac{\sqrt{1-q}}{z} \sum_{n \geq 0} (-1)^n q^{n(n+1)/2} \left(\frac{1 - \sqrt{1 - (4z^2/(1-q))}}{2z/\sqrt{1-q}} \right)^{2n+1} \quad (10)$$

$R(z, q)$ is first given in [16], which is closely related to the Stieltjes transform of the measure of continuous q -Hermite polynomial [17, 18]. (9) is equivalent to

$$\sum_{p \geq 1} m_p z^p = \left(1 + \frac{zR'(z, q)}{R(z, q)} \right) \frac{\lambda_1 z R(z, q)}{1 - \lambda_1 z R(z, q)} \quad (11)$$

where $R'(z, q) = \frac{dR(z, q)}{dz}$. This is because every decomposable structure admits an equivalent standard specification [19]. See the proof of the equivalence between (9) and (11) in section 3.1. We note that the generating function in (11) can be approximated by

$$\int_{-\infty}^{+\infty} \rho_{\text{extra}}(E) \frac{1}{1 - zE} dE \quad (12)$$

where $\rho_{\text{extra}}(E)$ is the approximated density of states corresponding to the moments m_p :

$$\rho_{\text{extra}}(E) = \left(\frac{E}{\lambda_1 R(1/E, q)} \right)' \delta \left(\frac{E}{\lambda_1 R(1/E, q)} - 1 \right). \quad (13)$$

One can show that (13) is obtained from (12) because of a simple identity

$$\int_{-\infty}^{+\infty} \frac{\delta(s-1)}{1-zs} ds = \frac{1}{1-z}.$$

Set $z = \lambda_1 z' R(z', q)$, then $z' \frac{dz}{dz'} = \lambda_1 z' R(z', q) \left(1 + \frac{z R(z', q)'}{R(z', q)}\right)$.

Furthermore, the Kronecker delta function in (13) gives us the location of the separated eigenvalue, which is the solution of the secular equation

$$\frac{E}{\lambda_1 R(1/E, q)} - 1 = 0. \quad (14)$$

We notice that (14) can only have a solution with $E > \frac{2}{\sqrt{1-q}}$ when $\lambda_1 > \lambda_1^c$ which will be identified in 4.1. For example, when $q = 0$, $R(z, 0) = \frac{1 - \sqrt{1-4z^2}}{2z^2}$, which is the generating function for the Catalan numbers. Therefore, (14) in this case can have a solution $\frac{1+\lambda_1^2}{\lambda_1}$ only when $\lambda_1 > 1$. This is exactly the same as the random matrix theory with shifted mean Gaussian entries [6, 7].

To conclude, the ensemble averaging density of (1) in the double scaled limit (3) is

$$\rho(E) = \begin{cases} \rho_0(E) + 2^{-\lfloor N/2 \rfloor} \delta(E - E_{\text{split}}) & \lambda_1 > \lambda_1^c \\ \rho_0(E) & \lambda_1 < \lambda_1^c \end{cases} \quad (15)$$

where E_{split} is the solution of (14) and $\rho_0(E)$ denotes the ensemble averaging density of SYK model in the double scaled limit (3), which is given by the weight function of Q-Hermite polynomial [11]

$$\rho_0(E) := \rho_{QH}(E) = c \sqrt{1 - \left(\frac{E}{2/\sqrt{1-q}}\right)^2} \prod_{k=1}^{\infty} \left[1 - 4 \left(\frac{E}{2/\sqrt{1-q}}\right)^2 \left(\frac{1}{2 + q^k + q^{-k}}\right) \right] \quad (16)$$

where c is a normalization constant such that $\int \rho_0(E) dE = 1$. Once we get E_{split} the location of the separated eigenvalue, the asymptotic expression of the moments m_p can be simplified significantly

$$m_p \simeq \lambda_1^p \sum_{j=0}^{\lfloor \frac{p-1}{2} \rfloor} \binom{p}{j} \left(\frac{E_{\text{split}}}{\lambda_1} - 1\right)^j \quad (17)$$

Both (7) and (17) are in closed agreement with the numerical results with fixed p , the comparisons between analytical and numerical results are given in section 5.

1.2 Plan of the paper

In section 2, we introduce briefly the basic combinatorial languages to be used throughout this paper. Section 3 is devoted to explaining in detail the mapping between moments calculation of m_p and the enumeration of certain combinatorial structures identified below. We collect results of m_p from analytic combinatorics. Section 4 contains the singularity analysis of the generating function of combinatorial structures. We further demonstrate how to locate the phase transition and the gap in the spectrum of (1) by using singularity expansions. Section 5 presents the comparison between our analytic expressions and the numerical results obtained by calculating the eigenvalues of (1) with Mathematica. Finally, in section 6, we give a brief conclusion and discuss the directions for further research.

2 Combinatorial structures and construction operators

First of all, a class of combinatorial structures is a set of objects with different sizes. The size of an object is the number of its nodes (components). In addition, the number of objects of each size is finite. The set is described by finite rules. In order to enumerate these objects with respect to their properties, these rules admit a direct translation as operations over generating functions of corresponding structures. On top of this, many combinatorial structures can be built by more elementary building blocks; this translate into generating function means that a decomposable structure has a functional composition scheme for its generation function. In the following we present some basic concepts about how to construct a combinatorial structure by putting more basic substructures together.

2.1 Labelling object

A labeled object means each of its nodes carries, whether with a distinctive color, or equivalently an integer label, in such a way that all the labels occurring in an object are distinct. So a labeled class is a collection of labeled objects with different sizes. An object is rooted if a particular node is specified, this node is known as the root. Therefore for a rooted structure \mathcal{A} , its generating function is

$$\mathcal{A} = \mathcal{Z} \times \mathcal{B} \implies A(z) = zB(z)$$

where \mathcal{Z} represents the root in \mathcal{A} , it is then attached to substructure \mathcal{B} . $A(z) = \sum_k a_k z^k$ and $B(z) = \sum_k b_k z^k$ are two generation functions enumerate structures \mathcal{A} and \mathcal{B} respectively (i.e. the coefficients a_k and b_k are the numbers of \mathcal{A} -structures and of \mathcal{B} -structures of size k respectively).

2.2 Construction operators

Let's consider two basic operations: cartesian product \times and sequence SEQ,

$$\mathcal{A} = \mathcal{B} \times \mathcal{C} \implies A(z) = B(z)C(z) \tag{18}$$

this means the cartesian product \mathcal{A} consists in forming all pairs with a first component in \mathcal{B} and a second component in \mathcal{C} .

$$\mathcal{A} = \text{SEQ}(\mathcal{B}) \implies A(z) = \frac{1}{1 - B(z)} \tag{19}$$

SEQ(\mathcal{B}) builds a sequence of component from \mathcal{B} . Next, consider a labeled cycle structure CYC(\mathcal{B}) := SEQ(\mathcal{B})/ \mathbf{S} , which is a set of cycles of labeled nodes; each node is attached to elementary building blocks \mathcal{B} up to the equivalence relation \mathbf{S} (i.e., a cycle is invariant

under the rotation), the corresponding generating function of $\text{CYC}(\mathcal{B})$ is

$$\mathcal{A} = \text{CYC}(\mathcal{B}) \implies A(z) = \sum_{k=1}^{\infty} \frac{B(z)^k}{k} = \log \frac{1}{1 - B(z)} \quad (20)$$

The final operation we need to construct our structure is the pointing operator Θ . It consists in pointing (or marking) one of the components along all the ones that compose an object of size n . Θ operator is equivalent to the differential operator in combinatorial differential calculus [10]. For a given structure \mathcal{B} of size n , the pointing of \mathcal{B} means that one of its n nodes is distinguished; hence, there are n different ways of pointing this structure. Consider a structure \mathcal{A} which can be decomposed by a pointing operator of a substructure \mathcal{B} , its generating function follows:

$$\mathcal{A} = \Theta \mathcal{B} \implies A(z) = z \frac{d}{dz} B(z) \quad (21)$$

see figure 1 for the illustration.

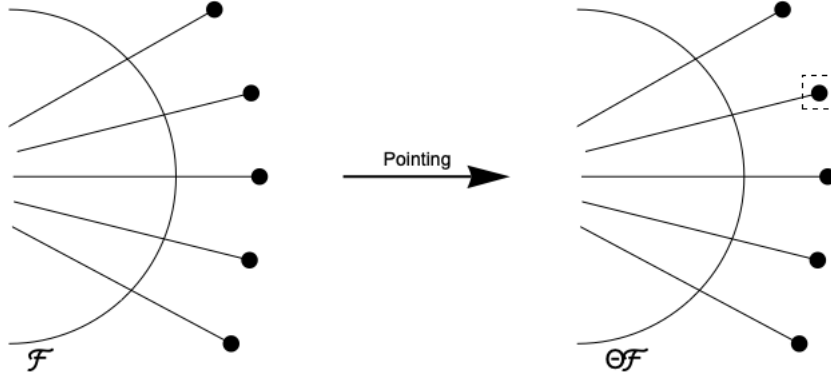


Figure 1: An example of pointing operator of a given structure \mathcal{F} with size 5: one of the 5 nodes is pointed by a dotted rectangle on the left side of the figure

2.3 Multitudinous combinatorial structure

Now consider a complex structure \mathcal{A} which is composed by a pointing operator of labeled cycles of a rooted substructure \mathcal{B} . Clearly,

$$\mathcal{A} = \Theta \text{CYC}(\mathcal{Z} \times \mathcal{B}) \implies A(z) = z \frac{d}{dz} \log \frac{1}{1 - zB(z)} \quad (22)$$

this leads to the enumeration of the \mathcal{A} -structures of size n

$$\begin{aligned} a_n &= n[z^n] \log \frac{1}{1 - zB(z)} \\ &= n \sum_{k_1+2k_2+3k_3+\dots=n} \frac{\binom{k_1+k_2+k_3+\dots}{k_1, k_2, k_3, \dots}}{k_1 + k_2 + k_3 + \dots} b_1^{k_1} b_2^{k_2} b_3^{k_3} \dots \end{aligned} \quad (23)$$

where $[z^n]$ denotes the coefficient of extraction of z^n in series expansion.

Now we illustrate the previous definitions by enumerating a pointed cycle of binary trees. The building block here is the binary tree, i.e. , a rooted plane tree with each node having two descendants; see figure 2 for some examples.

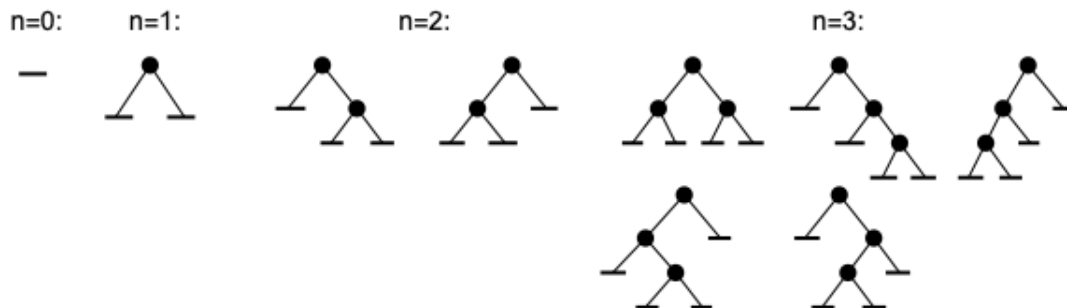


Figure 2: Binary trees with size $n = 0, 1, 2, 3$ with respective cardinalities 1, 1, 2, 5

The number of binary trees that have n branching nodes is given by Catalan number C_n and the corresponding generating function is

$$\begin{aligned}
 B(z) &:= \sum_{n \geq 0} C_n z^n \\
 &= \frac{1 - \sqrt{1 - 4z}}{2z}
 \end{aligned} \tag{24}$$

Now consider a pointed labeled cycle \mathcal{A} , which is a necklace with each labeled bead attached to a binary tree, i.e. the root of each tree connects directly to a labeled bead. Thus, according to (23), its generating function is

$$\begin{aligned}
 A(z) &:= \sum_{n \geq 1} a_n z^n \\
 &= z \frac{d}{dz} \log \frac{1}{1 - \frac{1 - \sqrt{1 - 4z}}{2}}
 \end{aligned} \tag{25}$$

where a_n is the number of such necklaces of size n . Therefore, by expanding (25), we get the enumeration of this complex structure. Figure (3) below shows an example of the enumeration of these necklaces with $n = 3$. Construction of a labeled necklace with 3 nodes in terms of binary trees: this necklace can either have

- 1 labeled bead attached to a binary tree with 3 nodes, therefore, it has 5 possibilities for the attachment (see the rightmost figure in Fig. 2).
- 2 labeled beads, one of them attached to a binary tree with 2 nodes (two possibilities for a binary tree of size 2; see the middle figure in Fig. 2) and the other attached to a binary tree with 1 node. In addition, since the necklace has two labeled beads, either of them can be attached to a binary tree of size 2. So we have double chances for labelling. Therefore, we have $2(2 \times 1) = 4$ possibilities to compose this necklace.

- 3 labeled beads, each of them attached exactly to 1 node. Since each bead is attached to the same structure, it is cyclic invariant under rotation. Therefore, we have exactly 1 way to make this necklace.

To sum up, the total number of labeled necklaces with 3 nodes in terms of binary trees is $5 + 4 + 1 = 10$, which equals exactly to $3[z^3] \log \frac{1}{1-zB(z)}$ with $B(z)$ in (24).

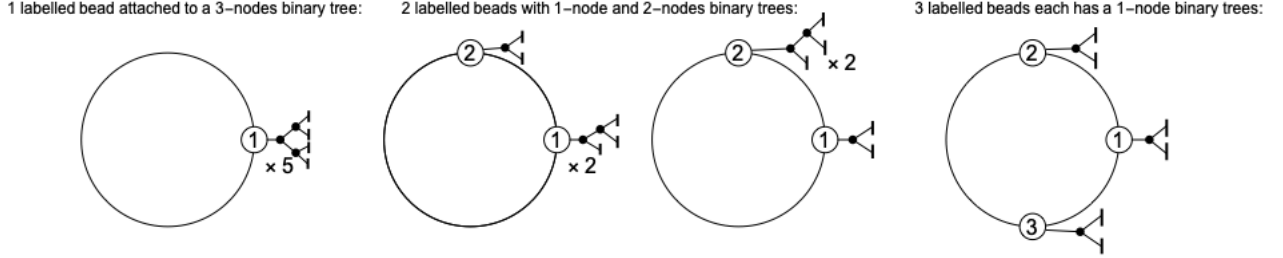


Figure 3: All the possible labeled necklaces of binary trees of size $n = 3$

In the following section, we study the mapping between the generating function of certain combinatorial class and moments calculation of quantum mechanics model (1)

$$\langle \text{tr} H^n \rangle_J = n[z^n] \log \frac{1}{1 - zB(z)} \quad (26)$$

with certain generating function $B(z)$ which will be identified later. Once we identify the specification of the combinatorial class, we can use singularity analysis of the corresponding generating function to locate the phase transition that happens in the eigenvalues distributions of (1).

3 Moments calculation

In this section, we discuss how to study the eigenvalue distribution of (1) by using analytic combinatorics [9] to construct a complex combinatorial structure. Our approach is first to map the ensemble averaging moments of (1) into a counting problem of complex combinatorial structures; then we can get an analytic expression from the combinatorial counting. It is important to remember that our calculation is under the double scaled limit (3). Our goal here is to calculate

$$m_p := 2^{\lfloor N/2 \rfloor} \left(\langle \text{tr}(H_{\text{SYK}} + \mathbb{A})^p \rangle_J - \langle \text{tr} H_{\text{SYK}}^{2\lfloor p/2 \rfloor} \rangle_J \right) \quad (27)$$

where p can be either even or odd nonzero integers. Let's recall that tr in this paper is normalized such that $\text{tr} \mathbb{A}^i = \lambda_1^i / 2^{\lfloor N/2 \rfloor}$ and $\langle \text{tr} H_{\text{SYK}}^{2j} \rangle_J = \text{RT}(j, q)$ with i and j being positive integers. Thus, we need to multiply the difference in (27) by $2^{\lfloor N/2 \rfloor}$ to get finite results in large N limit. Notice that the Hamiltonian of SYK can be treated as a sparse

matrix; therefore we can not expand (27) in terms of binomial coefficients. We can map the calculation of (27) into a counting problem of cyclic composition, since the trace of a matrix is invariant under cyclic permutation.

To begin with, the ensemble averaging operator $\langle \dots \rangle_J$ only affects H_{SYK} ; it forces all the H_{SYK} in (27) to appear in pairs since every independent J needs to appear exactly twice to obtain non-zero results after the ensemble averaging calculation. The pairing of all the H_{SYK} in (27) leads to a counting problem of perfect matching. Consequently, the contribution from H_{SYK} in (27) must be even. Thus one can represent $\langle \text{tr} H_{\text{SYK}}^k \rangle_J$ by enumerating chord diagrams. Each diagram is a circle with k even nodes. Each node represents an H_{SYK} insertion, then using chords to connect the nodes in pairs when two H_{SYK} share the same index set. Two chords are crossed when two pairs of H_{SYK} have some common elements in their sets of indices. See figure 4 for all the possible chord diagrams of size 4, this is enumerated by $\langle \text{tr} H_{\text{SYK}}^4 \rangle_J$. We refer to [5] for the details of the connection between chord diagram enumeration and moments calculation of the SYK Hamiltonian.

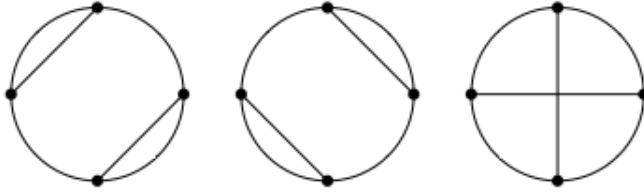


Figure 4: 3 possible chord diagrams of size 4

Secondly, because we are in large N limit, when we calculate the moments (27), we only count products of consecutive H_{SYK} , because the extra source Λ only has one nonzero entry λ_1 , the product of Λ sandwiched between any number of paired H_{SYK} can be neglected. This means (27) can be written in terms of $\langle \text{tr} H_{\text{SYK}}^i \rangle_J^{k_i}$ and $\lambda_1^{p - \sum_i i k_i}$ with integers $k_i \in [0, \lfloor (p-1)/2 \rfloor]$. Expanding (27) into its normally ordered form where all the $\langle \text{tr} H_{\text{SYK}}^{2i} \rangle_J$ are rearranged together following by all the λ_1 . Replacing $\langle \text{tr} H_{\text{SYK}}^{2i} \rangle_J$ by $\text{RT}(i, q)$, we have

$$\sum \text{RT}(1, q)^{k_1} \text{RT}(2, q)^{k_2} \dots \text{RT}(l, q)^{k_l} \dots \lambda_1^{p-2 \sum_i i k_i} \quad (28)$$

where the summation is over all the combinations of products of $\text{RT}(i, q)$ and λ_1 with different orders that satisfy the total exponent equals p . Besides, in (27), we subtract all the contributions only from SYK $\langle \text{tr} H_{\text{SYK}}^{2 \lfloor p/2 \rfloor} \rangle_J$. Accordingly, the exponent of λ_1 must be positive, then $2 \sum_i i k_i < p$. Now, in order to make a connection to combinatorial enumeration, we need to do some adjustments to this product. We first multiplied each $\text{RT}(i, q)$ by λ_1 ; then the exponent in λ_1^{p-2j} must be reduced to keep the product invariant

$$\sum (\lambda_1 \text{RT}(1, q))^{k_1} (\lambda_1 \text{RT}(2, q))^{k_2} \dots (\lambda_1 \text{RT}(l, q))^{k_l} \dots \lambda_1^{p-2 \sum_i i k_i - \sum_i k_i}. \quad (29)$$

Since each $\text{RT}(i, q)$ enumerates chord diagrams of size i according to the number of crossings [20, 21], the sum of all the possible normal forms above can be understood as an enumeration of a collection of chord diagrams with different sizes (including size 0) basing on the total number of crossings, it is additionally invariant under cyclic permutation. Thus, this can be mapped to a counting problem of necklaces with each labeled bead attached to a chord diagram (one of the nodes in each chord diagram contacts directly to a labeled bead; this node is called the root of the corresponding chord diagram). The multiplication of λ_1 in each parenthesis of (29) can be viewed as a marker for each occurrence of chord diagram. The rest $\lambda_1^{p-2\sum_i ik_i - \sum_i k_i}$ marks the bead attached to a 0-chord diagram (i.e. diagram with 0 nodes and $\text{RT}(0, q) = 1$). Such a necklace can have at most $2\lfloor(p-1)/2\rfloor$ nodes in the attached chord diagrams since we extract all the contributions that only come from SYK Hamiltonian. We need to label the beads, because the order of different $\text{RT}(i, q)$ contributed in (27) matters. An example of this kind of necklace is shown in Figure 5 with $p = 10$: bead 1 is attached to a chord diagrams of 2 nodes, bead 2 is attached to a chord diagrams of 4 nodes and 1 crossing, bead 3 is attached to 0-chord diagram, thus marked by $\lambda_1^{10-(2+4)-2} = \lambda_1^2$ (for simplification, we don't show the 0-chord diagram on the figure).

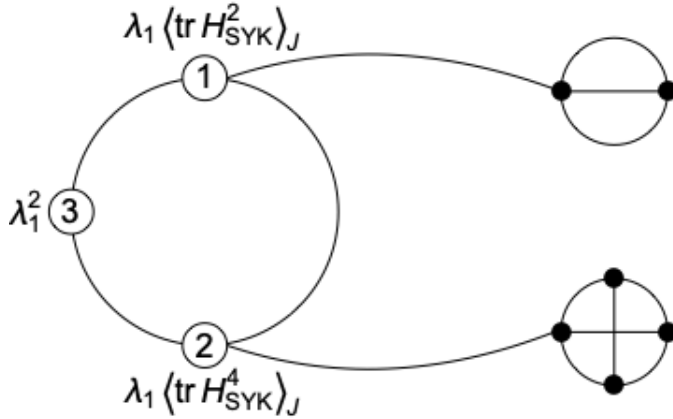


Figure 5: A necklace of labeled beads attached to 3 chord diagrams: bead 1 is attached to a 2-chord diagram; bead 2 is attached to a 4-chord diagram and bead 3 is attached to a 0-chord diagram

More precisely, the connection between the calculation of (27) and the enumeration of the combinatorial structures described above is given by

$$m_p = \sum_{\pi \in \mathcal{N}_{cd}} q^{\#\text{crossing}} \quad (30)$$

where π represents a specific labeled necklace of size p composed of chord diagrams. Once we have this mapping, we can use the trick introduced in section 2 to get the enumeration of the right hand side of (30), or equivalently, the subtracted moments (27).

3.1 Hanging chord diagrams in necklaces

A labeled necklace of chord diagrams is a necklace of beads on which chord diagrams are hung on and all the beads are labeled by integers. We denote by \mathcal{N}_{cd} the set of such necklaces. The building blocks here are the chord diagrams, we denote it by \mathcal{CD} . In addition, we use λ_1 to mark each of them. Thus,

$$\mathcal{N}_{cd} = \Theta \text{CYC}(\lambda_1 \mathcal{Z} \times \mathcal{CD}) \quad (31)$$

\mathcal{Z} represents the root of a chord diagram (the node connected to a bead). The cyclic structure comes from the fact that a necklace is invariant by rotation. From (22), we get its generating function

$$\begin{aligned} N_{cd}(z) &:= \sum_{p \geq 1} N_p z^p \\ &= z \frac{d}{dz} \log \frac{1}{1 - \lambda_1 z R(z, q)} \end{aligned} \quad (32)$$

where N_p is the number of such necklaces with maximal $p - 1$ nodes. N_p enumerates the right hand side of (30). $R(z, q)$ is given by (10), which is the generating function of the chords diagrams enumeration.

We can reduce cycles to sequences

$$\mathcal{A} = \text{CYC}(\mathcal{B}) \quad \Rightarrow \quad \Theta \mathcal{A} = \mathcal{C} \times \Theta \mathcal{B}, \quad \text{with } \mathcal{C} = \text{SEQ}(\mathcal{B}). \quad (33)$$

This means a pointed cycle \mathcal{A} of substructures \mathcal{B} decomposes into the pointed component and the rest of the cycle; the directed cycle can then be opened at the place designated by the pointing \mathcal{B} and a sequence of \mathcal{B} . Therefore, combining (18), (19), (20), (21) and (33), we get

$$N_{cd}(z) = \left(1 + \frac{z R'(z, q)}{R(z, q)} \right) \frac{\lambda_1 z R(z, q)}{1 - \lambda_1 z R(z, q)}. \quad (34)$$

Since we know the mapping between moments calculation (27) and N_p , we prove our results (9), (11) and the equivalence between them. Now by expanding (34) or equivalently (32) and using (23), it follows that

$$\begin{aligned} N_p &:= [z^p] N_{cd}[z] \\ &= p \sum_{j=0}^{\lfloor \frac{p-1}{2} \rfloor} \sum_{\substack{k_1, k_2, \dots, k_j \geq 0 \\ k_1 + 2k_2 + \dots + jk_j = j}} \lambda_1^{p-2j-\sum_i k_i} \frac{\binom{p-2j}{k_1, k_2, \dots, k_j, p-2j-\sum_i k_i}}{p-2j} \prod_{i=1}^j (\lambda_1 \text{RT}(i, q))^{k_i} \end{aligned} \quad (35)$$

Therefore, by virtue of (30), we prove (7) through the mapping.

4 Singularity analysis of generating function

In this section, we borrow some important notions from analytic combinatorics [9] which will be used later to identify the radius of convergence and the singular exponents of our composition structures. Our goal here is to investigate the effect of the input λ_1 on the spectrum of (1) by using the singularity analysis of generating function (34). This means we need to locate its singularities and find the corresponding singular exponents. In order to do that, we consider λ_1 as a variable. The idea here is that this auxiliary variable is regarded as inducing a deformation of the original univariate generating function (i.e. (34) with $\lambda_1 = \lambda_1^c$, which will be identified later). This deformation can be analyzed by the corresponding asymptotic expansion of the generating function near its dominant singularities with a given λ_1 . Therefore, (34) becomes a bivariate generating function [9, Chapter III], we rewrite it as

$$\begin{aligned} N_{cd}(z, \lambda_1) &= \sum_{p,k} N_{p,k} z^p \lambda_1^k \\ &= \left(1 + \frac{zR'(z, q)}{R(z, q)}\right) \frac{\lambda_1 z R(z, q)}{1 - \lambda_1 z R(z, q)}. \end{aligned} \quad (36)$$

where $N_{p,k}$ is the number of necklaces in class \mathcal{N}_{cd} of size p having k components of rooted chord diagrams $\mathcal{Z} \times \mathcal{CD}$ (31). We call z and λ_1 the primary and the secondary variable of $N_{cd}(z, \lambda_1)$, respectively. It is easy to see that

$$N_p(\lambda_1) := \sum_k N_{p,k} \lambda_1^k \equiv [z^p] N_{cd}(z, \lambda_1) \quad (37)$$

4.1 Singular expansions

We start by finding out where the singularities are located. As noted in (33), we can treat (36) as a product of two parts. Apparently, the sequence part \mathcal{C} with the corresponding generating function

$$C(z, \lambda_1) = \frac{1}{(1 - \lambda_1 z R(z, q))} \quad (38)$$

has singularities at $\rho_C(\lambda_1)$ satisfying

$$\rho_C(\lambda_1) R(\rho_C(\lambda_1), q) = 1/\lambda_1. \quad (39)$$

The rest part of (36) has constant singularities with given q , which does not change with λ_1 . Therefore, we only need to focus on $\rho_C(\lambda_1)$ and its influence on (38) to study the perturbations induced by λ_1 .

Let's consider (38) as a functional composition of two functions analytic at the origin that have non-negative coefficients

$$C(z, \lambda_1) = f(\lambda_1 g(z)) \quad \text{with} \quad f(z) = \frac{1}{1-z} \quad \text{and} \quad g(z) = zR(z, q). \quad (40)$$

Let ρ_g, ρ_f be the radii of convergence of $g(z)$ and of $f(z)$, and define

$$\tau_g = \lim_{z \rightarrow \rho_g^-} g(z) \quad \text{and} \quad \tau_f = \lim_{z \rightarrow \rho_f^-} f(z) \quad (41)$$

The singular expansion of (38) depends on the values of ρ_f, τ_g and λ_1 . $C(z, \lambda_1)$ is called critical if it satisfies $\lambda_1 \tau_g = \rho_f \equiv 1$. In this case, there is a confluence of singularities at $\rho_C = \rho_g$. Therefore, the collection of singular expansions is parameterized by λ_1 ⁵. In the following, we will show that there exist discontinuities in the singular behavior of (38) when the secondary parameter λ_1 traverses the special value λ_1^c .

By looking at the definition of $R(z, q)$ in (10), we find that $\rho_g = \sqrt{1-q}/2$ and the asymptotic of $g(z)$ around ρ_g is

$$\begin{aligned} g(z) &\sim \tau_g + c_g \sqrt{1 - \frac{z}{\rho_g}} \quad \text{with } c_g < 0 \\ \text{and } \tau_g &= \sqrt{1-q} \sum_{k \geq 0} (-1)^k q^{k(k+1)/2} \end{aligned} \quad (42)$$

Since $q \in [0, 1]$, τ_g is less than or equal to 1. We distinguish 3 cases of singular expansion of (38) by the values of λ_1

- Obviously, (38) is critical at

$$\rho_C = \rho_g = \sqrt{1-q}/2 \quad \text{if} \quad \lambda_1 = \lambda_1^c := \frac{1}{\sqrt{1-q} \sum_{k \geq 0} (-1)^k q^{k(k+1)/2}} \quad (43)$$

we find the local singular expansion

$$C(z, \lambda_1^c) \sim \left(\frac{-\lambda_1^c c_g}{\rho_f} \right)^{-1} \frac{1}{\sqrt{1 - z/\rho_g}} \quad \text{where } \rho_f \equiv 1 \quad (44)$$

- When $\lambda_1 < \lambda_1^c$, we call it subcritical. In this case, $f(\lambda_1 z)$ is analytic at τ_g . It is such that the perturbations induced by the λ_1 affect neither the location nor the nature of the basic singularity of (38). In this case, $\rho_C = \rho_g = \sqrt{1-q}/2$ is constant, which does not change with λ_1 . On that basis expansions show that

$$C(z, \lambda_1) \sim f(\lambda_1 \tau_g) - c \lambda_1 f'(\lambda_1 \tau_g)(\lambda_1) \sqrt{1 - \frac{z}{\rho_g}} \quad \text{with a constant } c \in \mathbb{R}^+ \quad (45)$$

- When $\lambda_1 > \lambda_1^c$, we call it supercritical. In this case, $f(\lambda_1 z)$ is also analytic at τ_g . Furthermore, there exists a value r with $r < \rho_g$ such that $\lambda_1 g(r)$ attains the value ρ_f , which triggers a singularity of $C(z, \lambda_1)$. In other words, $r \equiv \rho_C$ and ρ_C here is no longer constant, it is the solution of (39). Since around this point, $g(z)$ is analytic, the singular expansion of $C(z, \lambda_1)$ can be obtained by combining the singular expansion of $f(z)$ with the regular expansion of $g(z)$ at $r = \rho_C(\lambda_1)$

$$C(z, \lambda_1) \sim -\frac{1}{\lambda_1 g'(r)} (z - r)^{-1} \quad \text{where } r \text{ is a solution of (39)} \quad (46)$$

⁵we refer [9, Chapter VI] for a more detailed presentation of singular expansions of functional composition.

To conclude the three situations above, not only does the location of the singularity $\rho_C(\lambda_1)$ change with λ_1 , but the corresponding singular exponent $\alpha_C(\lambda_1)$ also changes as λ_1 increases and crosses the critical value λ_1^c . They both experienced a non-analytic transition at λ_1^c . We use a simple diagram to visualize changes in the singularity $\rho_C(\lambda_1)$ and the corresponding singular exponent $\alpha_C(\lambda_1)$, it is called phase-transition diagram [9, Chapter IX]

$$\begin{array}{cccc|c} \lambda_1 & \lambda_1^c - \epsilon & \lambda_1^c & \lambda_1^c + \epsilon & \\ \hline \rho_C & \frac{\sqrt{1-q}}{2} & \frac{\sqrt{1-q}}{2} & r & Z := \rho_C - z \\ \hline Z^{\alpha_C(\lambda_1)} & Z^{1/2} & Z^{-1/2} & Z^{-1} & \end{array}$$

Thus, the location of the phase transition is at λ_1^c . In the following we use the results above to find the gap in the spectrum of (1).

4.2 Locating the gap

Here, we only need to consider the supercritical case since the gap in the spectrum of (1) only appears when $\lambda_1 > \lambda_1^c$. The singular expansion of (36) in this case is a product of (46) and the singular expansion of $\lambda_1 z g'(z)$ around $z = r$. Because $g(z)$ is analytical at r , the singular expansion of (36) around $z = r$ can be written as

$$N_{cd}(z, \lambda_1) \sim \frac{1}{1 - z/r} \quad (47)$$

Then we can use a simple identity

$$\int_{-\infty}^{+\infty} \frac{\delta(s - a)}{1 - zs} ds = \frac{1}{1 - az}$$

to identify the corresponding density of states $\rho(E)$ satisfying

$$\int_{-\infty}^{+\infty} \rho(E) \frac{1}{1 - zE} dE = \frac{1}{1 - z/r}$$

it gives

$$\rho(E) = \delta(E - 1/r)$$

Therefore, the gap is located at $1/r$ with r being the solution of (39) and consequentially we get (14) from (39) via Stieltjes transform.

As we demonstrated in this section, the perturbations induced by λ_1 display as the discontinuities in singular behavior of (36). It causes the phase transition in combinatorial counting and therefore causes the phase transition in the spectrum of (1) via the specific mapping identified in section 4.

5 Numerical comparison

We compare our analytic expressions with numerical results of (1) at finite N and fixed $q = 4$. Although all the expressions obtained in this paper are under the double scaled

limit (3), they are still good approximations to the exact results for fixed $q \ll N$. The reason for this is that SYK model itself has a very good agreement between the double scaled analytic expressions and its exact numerical results for finite fixed q , even for low values of N [11]. We won't discuss the calculation of the p -dependent corrections here. We refer to [5, 13] for more details about how to calculate analytically the difference between fixed p case and the double scaled limit. In the following, we first test the correctness of our moments expressions (7) and (17). Then we show numerical evidence of a phase transition that happens in spectral density when λ_1 passes its critical values λ_1^c . Finally, we compare the numerical results of the single eigenvalue which is split from the SYK spectrum when $\lambda_1 > \lambda_1^c$ with our analytic prediction (14).

We use Mathematica to calculate the eigenvalues of (1) with input $\lambda_1 = 3$ and 50 samplings. Figure (6) shows the moments m_p of $N = 26$, $N = 28$, $N = 30$ and $N = 32$ respectively. The numerical results are obtained by using these eigenvalues calculated by Mathematica and after spectral and ensemble averaging of the samples. Since we are comparing our analytical expressions with numerical results of the $p = 4$ case, we need to replace all the q in (7) and (17) by $\tilde{q}(4)$ where $\tilde{q}(p)$ is defined by (6).

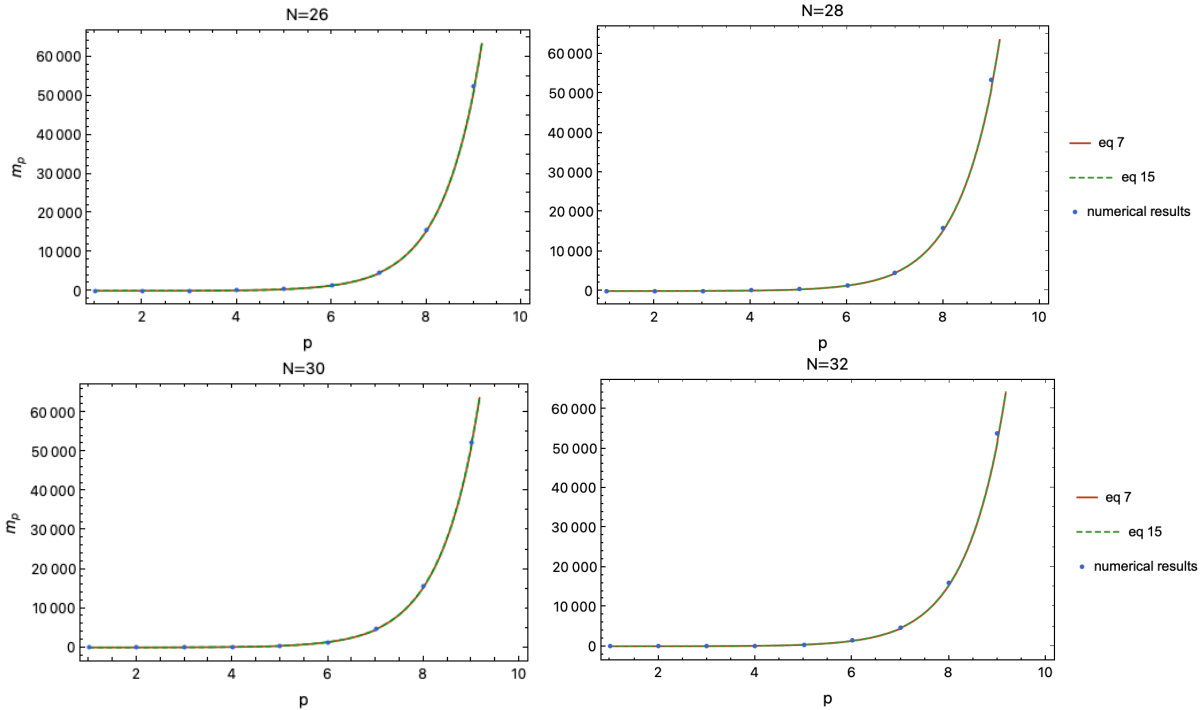


Figure 6: Moments calculations comparison: the blue disk corresponds to the numerical results after spectral and ensemble average of 50 samples. The red solid line is the analytical prediction (7). The green dashed line is the analytical prediction (17)

As shown above, for the first few moments, we have excellent agreement between (7), (17) and with numerical calculations.

Figure 7 below shows two examples ($N = 24$ and $N = 26$) of empirical spectral

measure of (1) with two different values of λ_1 . As λ_1^c defined in (43), for both $N = 24$ and $N = 26$ cases, $\lambda_1 = 1$ is smaller than λ_1^c and $\lambda_1 = 3$ is larger than λ_1^c . One can see that as λ_1 passes its critical values, there is a gap that appears in the spectrum. The main spectrum can be approximated by analytical expression of SYK's spectral density $\rho_{QH}(E)$ (16). With given $\lambda_1 > \lambda_1^c$, the single split eigenvalue moves with N ; hence it depends on q as we predicted in the previous section.

In the following, we list the comparison between the numerical results and the analytic prediction of the averaged single split eigenvalue or $N = 24, N = 26, N = 28, N = 30$ and $N = 32$:

| N | $\langle E_{\text{split}}^{\text{numer}} \rangle$ | $E_{\text{split}}^{\text{analy}}$ | σ_{split} |
|-----|---|-----------------------------------|-------------------------|
| 24 | 3.33851005 | 3.33824460 | 0.0620565 |
| 26 | 3.34104622 | 3.33979434 | 0.0612582 |
| 28 | 3.34994743 | 3.34131759 | 0.0508209 |
| 30 | 3.34204363 | 3.34280205 | 0.0508951 |
| 32 | 3.35162725 | 3.34424154 | 0.0599583 |

where $\langle E_{\text{split}}^{\text{numer}} \rangle$ are the sample means of numerical results of the split eigenvalue. Each sample has exactly one split eigenvalue, we denote the single split eigenvalue in the i -th sample by E_i^{split} . Thus, $\langle E_{\text{split}}^{\text{numer}} \rangle = \frac{1}{50} \sum_{i=1}^{50} E_i^{\text{split}}$. Analytic prediction of this single split eigenvalue $E_{\text{split}}^{\text{analy}}$ is given by(14). σ_{split} in the table test the deviation of the sampling E_i^{split} away from the analytical prediction $E_{\text{split}}^{\text{analy}}$, defined as

$$\sigma_{\text{split}} = \sqrt{\frac{1}{50} \sum_{i=1}^{50} (E_i^{\text{split}} - E_{\text{split}}^{\text{analy}})^2}$$

In this section we have checked that our analytic expressions are in good agreement with those calculated numerically from the exact diagonalization of (1) with $p = 4$ and finite N . It should be noticed that our analytical results also work fine for other p fixed cases such as $p = 3$.

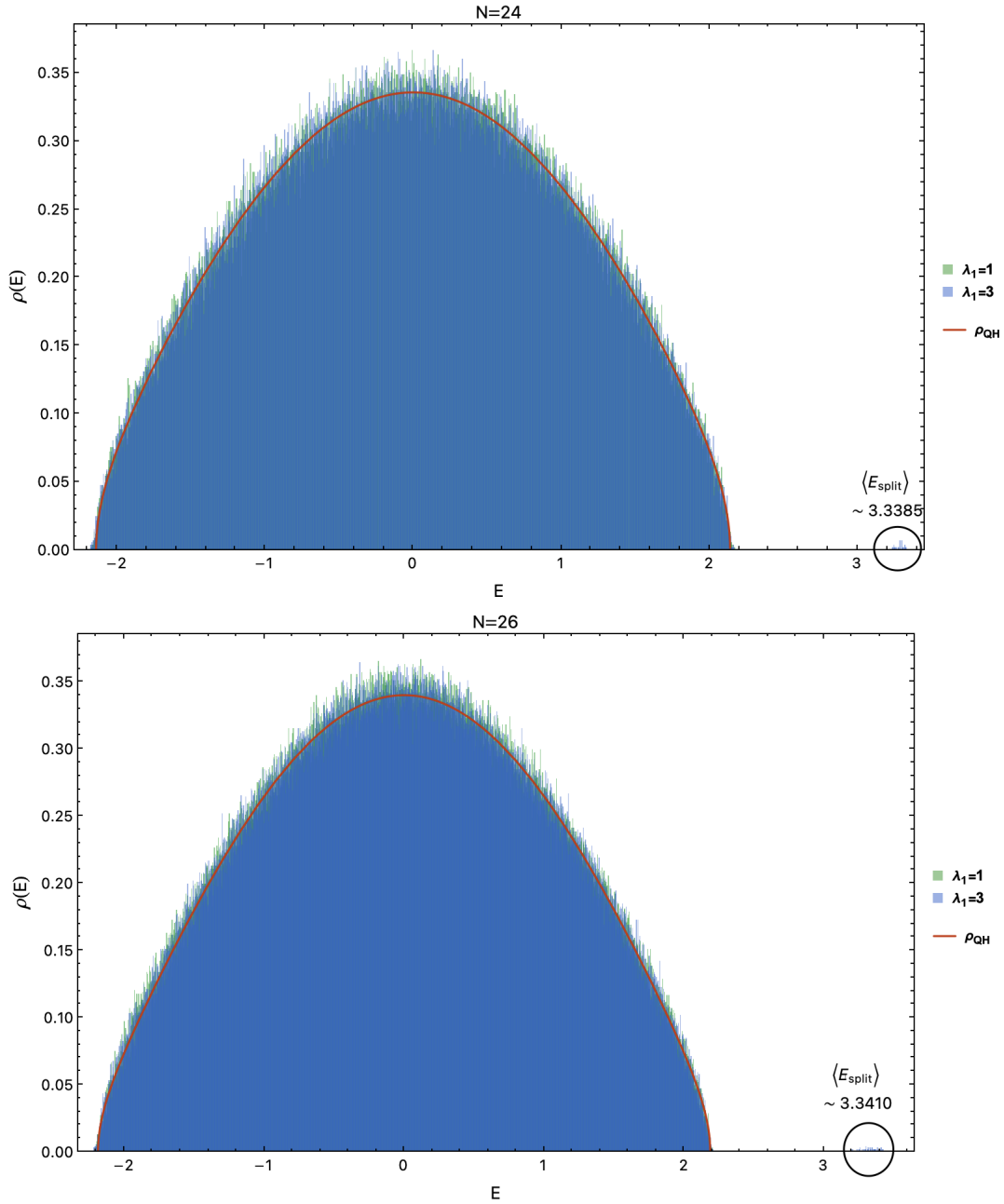


Figure 7: Comparison of the numerical spectral density of (1) with $p = 4$, $\lambda_1 = 1$ (green shaded histogram) and $\lambda_1 = 2$ (blue shaded histogram) for $N = 24$ and $N = 26$, obtained by normalised histograms of eigenvalues of (1) with sample size 50, with the analytical prediction of the SYK spectral density $\rho_{QH}(E)$ (red smooth line). The sample mean of single split eigenvalue equals 3.3385 for $N = 24$ (circled on the top figure) and equals 3.3410 for $N = 26$ (circled on the bottom figure).

6 Conclusion

We have studied (1) an SYK-like model with an extra part, which is a simple diagonal matrix with only one non-zero entry λ_1 . This model can be understood as an SYK model “poisoned” by a rank 1 perturbation. Our analytic results not only are exact in the double scaled limit (3) but also are compatible with the p fixed and N finite cases. We have used the methods from analytic combinatorics to study the eigenvalue distribution of this model. Based on this, we have found that there is a phase transition in the secondary parameter λ_1 such that when λ_1 passes its critical value λ_1^c , a gap appears in the spectrum and a single eigenvalue splits outside the ensemble averaging SYK spectral density. We identified this eigenvalue by using singular analysis of a generating function which enumerates a specific class of combinatorial structures. The prime goal of our work is to better understand the precise effect of adding a deformation to the SYK Hamiltonian has on its eigenvalue distribution. Since (1) only adds the smallest rank of perturbation, it can be used as a toy model to test the mapping between the phase transitions in physics and in combinatorial enumerations. Further research on more complicated higher rank perturbations can be built from here.

7 Acknowledgments

We would like to thank Antonio M. García-García for the interesting discussion, useful suggestions and for a careful reading of the manuscript. We also acknowledge discussions with Hanteng Wang. More particularly, we would like to thank Stephan Wagner for communicating the derivations in the appendix.

Appendix

We would like to have a closed form for the sum

$$S(p, j) = \sum_{\substack{k_1, k_2, \dots, k_j \geq 0 \\ k_1 + 2k_2 + \dots + jk_j = j}} \binom{k_1 + k_2 + \dots + k_j}{k_1, k_2, \dots, k_j} \binom{p - 2j}{k_1 + k_2 + \dots + k_j} \prod_{i=1}^j C_i^{k_i},$$

where $C_i = \frac{1}{i+1} \binom{2i}{i}$ is a Catalan number. Let us first split the sum according to the value of $k_1 + k_2 + \dots + k_j$:

$$\begin{aligned} s(p, j, r) &= \sum_{\substack{k_1, k_2, \dots, k_j \geq 0 \\ k_1 + 2k_2 + \dots + jk_j = j \\ k_1 + k_2 + \dots + k_j = r}} \binom{k_1 + k_2 + \dots + k_j}{k_1, k_2, \dots, k_j} \binom{p - 2j}{k_1 + k_2 + \dots + k_j} \prod_{i=1}^j C_i^{k_i} \\ &= \sum_{\substack{k_1, k_2, \dots, k_j \geq 0 \\ k_1 + 2k_2 + \dots + jk_j = j \\ k_1 + k_2 + \dots + k_j = r}} \binom{r}{k_1, k_2, \dots, k_j} \binom{p - 2j}{r} \prod_{i=1}^j C_i^{k_i}, \end{aligned}$$

so that

$$S(p, j) = \sum_{r=0}^j s(p, j, r).$$

We can rewrite $s(p, j, r)$ as follows:

$$s(p, j, r) = \frac{(p-2j)!}{(p-2j-r)!} \sum_{\substack{k_1, k_2, \dots, k_j \geq 0 \\ k_1 + 2k_2 + \dots + jk_j = j \\ k_1 + k_2 + \dots + k_j = r}} \prod_{i=1}^j \frac{C_i^{k_i}}{k_i!}.$$

The sum is exactly the coefficient of $x^j y^r$ in the expansion of

$$\prod_{i \geq 1} \sum_{k_i \geq 0} \frac{x^{ik_i} y^{k_i} C_i^{k_i}}{k_i!},$$

so we have

$$\begin{aligned} s(p, j, r) &= \frac{(p-2j)!}{(p-2j-r)!} [x^j y^r] \prod_{i \geq 1} \sum_{k_i \geq 0} \frac{x^{ik_i} y^{k_i} C_i^{k_i}}{k_i!} \\ &= \frac{(p-2j)!}{(p-2j-r)!} [x^j y^r] \prod_{i \geq 1} \exp(x^i y C_i) \\ &= \frac{(p-2j)!}{(p-2j-r)!} [x^j y^r] \exp\left(y \sum_{i \geq 1} x^i C_i\right) \\ &= \frac{(p-2j)!}{(p-2j-r)! r!} [x^j] \left(\sum_{i \geq 1} x^i C_i\right)^r \\ &= \binom{p-2j}{r} [x^j] \left(\sum_{i \geq 1} x^i C_i\right)^r. \end{aligned}$$

Thus

$$\begin{aligned} S(p, j) &= \sum_{r=0}^j \binom{p-2j}{r} [x^j] \left(\sum_{i \geq 1} x^i C_i\right)^r \\ &= [x^j] \sum_{r=0}^{p-2j} \binom{p-2j}{r} \left(\sum_{i \geq 1} x^i C_i\right)^r \\ &= [x^j] \left(1 + \sum_{i \geq 1} x^i C_i\right)^{p-2j}. \end{aligned}$$

Note here that we are allowed to include terms with $r > j$ in the sum since the lowest power of x in $\left(\sum_{i \geq 1} x^i C_i\right)^r$ is x^r , so that these terms do not actually contribute to the coefficient of x^j .

The generating function of the Catalan numbers is well known to be

$$F(x) = \sum_{i \geq 1} x^i C_i = \frac{1 - 2x - \sqrt{1 - 4x}}{2x},$$

it satisfies the implicit equation $F(x) = x(1 + F(x))^2$. Therefore, we can apply the Lagrange-Bürmann formula to obtain

$$\begin{aligned} S(p, j) &= [x^j](1 + F(x))^{p-2j} = \frac{1}{j} [t^{j-1}](p-2j)(1+t)^{p-2j-1}(1+t)^{2j} \\ &= \frac{p-2j}{j} [t^{j-1}](1+t)^{p-1} = \frac{p-2j}{j} \binom{p-1}{j-1} = \frac{p-2j}{p} \binom{p}{j}. \end{aligned}$$

References

- [1] S. Sachdev and J. Ye, Gapless spin-fluid ground state in a random quantum Heisenberg magnet, Phys. Rev. Lett. 70 (1993) 3339 [cond-mat/9212030].
- [2] S. Sachdev, Holographic metals and the fractionalized Fermi liquid, Phys. Rev. Lett. 105(2010) 151602 [1006.3794].
- [3] A. Kitaev, A simple model of quantum holography.
<http://online.kitp.ucsb.edu/online/entangled15/kitaev/>,
<http://online.kitp.ucsb.edu/online/entangled15/kitaev2/>.
- [4] T. Micklitz, Felipe Monteiro and A. Altland, Nonergodic extended states in the Sachdev-Ye-Kitaev Model, Phys. Rev. Lett. 123, 125701 (2019). [arXiv:1901.02389].
- [5] M. Berkooz, M. Isachenkov, V. Narovlansky and G. Torrents, Towards a full solution of the large N double-scaled SYK model, JHEP 03 (2019) 079 [arXiv:1811.02584].
- [6] S. F. Edwards and R. C. Jones, The eigenvalue spectrum of a large symmetric random matrix, J. Phys. A: Math. Gen., Vol. 9, No. 10, 1976
- [7] R. C. Jones, J. M. Kosterlitz and D. J. Thouless, The eigenvalue spectrum of a large symmetric random matrix with a finite mean, J. Phys. A: Math. Gen., Vol. 11, No. 3, 1978.
- [8] C. Banderier, M. Kuba, and M. Wallner, Phase transitions of composition schemes: Mittag-leffler and mixed poisson distributions. 2021 [arXiv:2103.03751].
- [9] P. Flajolet and R. Sedgewick, Analytic Combinatorics. Cambridge University Press, 2009.
- [10] P. Leroux and X.G. Viennot, Resolution combinatoire des systimes d'equations differentielles, II: calcul inttgral combinatoire, Ann. Sci. Math. QuCbec 12(2) (1988), 233-253.

- [11] A. M. García-García and J. J. M. Verbaarschot, Analytical Spectral Density of the Sachdev-Ye-Kitaev Model at finite N , Phys. Rev. D96 (2017) 066012 [arXiv:1701.06593].
- [12] A. M. García-García, Y. Jia and J. J. M. Verbaarschot, Exact moments of the Sachdev-Ye-Kitaev model up to order $1 = 1/N^2$, JHEP 04 (2018) 146 [arXiv:1801.02696].
- [13] Y. Jia and J. J. M. Verbaarschot, Large N expansion of the moments and free energy of Sachdev-Ye-Kitaev model, and the enumeration of intersection graphs, JHEP 11 (2018) 031 [arXiv:1806.03271].
- [14] L. Erdős and D. Schröder, Phase transition in the density of states of quantum spin glasses, Mathematical Physics, Analysis and Geometry 17 (2014) 441 [arXiv:1407.1552].
- [15] S. Ouvry, S. Wagner and S. Wu, On the algebraic area of lattice walks and the Hofstadter model, J. Phys. A: Math. Theor. 49 (2016) 495205 (22pp) [arXiv:1606.03273]
- [16] A. Cappelli and F. Colomo Solving the frustrated spherical model with q -polynomials, 1998 J. Phys. A: Math. Gen. 31 3141 [arXiv:hep-th/9710071]
- [17] J. Bustoz and M. E. H. Ismail, The associated ultraspherical polynomials and their q -analogues, Canadian J. Math. 34 (1982), 718-736.
- [18] M. E. H. Ismail, Classical and Quantum Orthogonal Polynomials in One Variable. Cambridge University Press, Cambridge, 2009.
- [19] P. Flajolet, P. Zimmerman and B. V. Cutsem, A calculus for the random generation of labeled combinatorial structures, Theoretical Computer Science 132 (1994) 1-35
- [20] J. Riordan, The distribution of crossings of chords joining pairs of 2 points on a circle, Mathematics of Computation 29 (1975), no. 129 215–222.
- [21] J. Touchard, Sur un probleme de configurations et sur les fractions continues, Canad. J. Math. 4 (1952), 2-25.